Copy
RM L54H13a

NACA

RESEARCH MEMORANDUM

A FLIGHT INVESTIGATION OF THE TRANSONIC AREA RULE FOR A 52.5° SWEPTBACK WING-BODY CONFIGURATION AT MACH NUMBERS BETWEEN 0.8 AND 1.6

By Sherwood Hoffman

Langley Aeronautical Laboratory
Langley Field, Va.

NATIONAL ADVISORY COMMITTEE
FOR AERONAUTICS

WASHINGTON

November 19, 1954

NATIONAL ADVISORY COMMITTEE FOR AERONAUTICS

RESEARCH MEMORANDUM

A FLIGHT INVESTIGATION OF THE TRANSONIC AREA RULE FOR A 52.5° SWEPTBACK WING-BODY CONFIGURATION AT MACH NUMBERS BETWEEN 0.8 AND 1.6

By Sherwood Hoffman

SUMMARY

An investigation of the transonic area rule has been conducted by zero-lift flight tests of models of a 52.5° sweptback wing-body configuration with and without a fuselage indentation and of equivalent bodies of revolution through a range of Mach number from 0.8 to 1.6 and Reynolds number from 4×10^6 to 12×10^6, based on wing mean aerodynamic chord. The wing had an angle of sweepback of 52.5° along the quarter-chord line, an aspect ratio of 3.0, a taper ratio of 0.2, and an NACA 65A004 airfoil section in the free-stream direction. The parabolic body had a fineness ratio of 10.

Indenting the fuselage of the wing-body combination, in order to reduce the normal cross-sectional area distribution to that of the original body alone, reduced the drag rise between Mach numbers 0.9 and 1.35 and increased the drag rise above Mach number 1.35. Near Mach number 1.0, approximately the same drag rise was obtained from the indented-body—wing combination and its equivalent body of revolution. The drag rise from the equivalent body of revolution with the bump corresponding to the wing was only 60 percent of that for the basic wing-body configuration at the speed of sound. The equivalent bodies did not indicate the pressure drag of the wing-body configurations at supersonic speeds.

INTRODUCTION

The design of high-speed aircraft for minimum drag rise near the speed of sound has been greatly enhanced by the concepts of the transonic area rule of reference 1. Investigations of the area rule by wind-tunnel tests and rocket-model tests (refs. 1 to 7) of research configurations and airplane configurations have shown that the drag rise near Mach number 1.0 varied approximately with the distribution of cross-sectional

area of the configurations. Tests of several configurations (refs. 2 and 6, for example) have shown that by modifying the configuration so that the resulting area distribution was conducive to low pressure drag, it was possible to reduce the drag at both transonic and low supersonic speeds. Because there is little information available at present regarding the Mach number limitations of this design concept, additional tests are being conducted to study the concepts of the area rule in more detail.

This paper presents the results of an investigation of the application of the transonic area rule for a basic configuration consisting of a 52.5° sweptback wing of aspect ratio 3.0 and taper ratio 0.2 on a parabolic body. The fuselage was modified with an axially symmetrical indentation to reduce the cross-sectional area of the basic configuration to that of the parabolic body alone. Tests also were made of equivalent bodies of revolution of the basic and modified wing-body combinations to check the concepts of the transonic area rule.

The flight tests covered continuous ranges of Mach number varying between 0.8 and 1.6. The corresponding Reynolds numbers varied between approximately 4×10^6 to 12×10^6, based on the mean aerodynamic chord of the wing.

SYMBOLS

A	cross-sectional area, sq in.
a	tangential acceleration, ft/sec^2
C_D	total drag coefficient, based on S_w
C_{D_f}	total drag coefficient, based on S_f
$\bar{c}$	mean aerodynamic chord of wing, ft
c	local wing chord, ft
g	acceleration due to gravity, 32.2 ft/sec^2
L	length of body, in.
M	free-stream Mach number
q	free-stream dynamic pressure, lb/sq ft
R	Reynolds number, based on $\bar{c}$

S_w total plan-form area of wing, sq ft

S_f frontal area of parabolic body, sq ft

W weight of model during deceleration, lb

x station measured from body nose, in.

γ angle between flight path and horizontal, deg

MODELS

Details and dimensions of the models tested are given in figure 1 and tables I to IV. The normal cross-sectional area distributions and photographs of the models are presented in figures 2 and 3, respectively.

The basic configuration, model A, consisted of a 52.5° sweptback wing on a parabolic body with four stabilizing fins. The parabolic body was formed from two parabolas of revolution joined at the maximum diameter (40-percent station) and had an overall fineness ratio of 10.0. The wing had an angle of sweepback of 52.5° along the quarter-chord line, an aspect ratio of 3.0 (based on total wing plan-form area), a taper ratio of 0.2, and an NACA 65A004 airfoil section in the free-stream direction. The ratio of total wing plan-form area to body frontal area was 16.5. Model B, which consisted of the wing on the body with an axially symmetrical indentation, had the same distribution of cross-sectional area as the parabolic body alone or model C. Models D and E were designed to be equivalent bodies of revolution having the same distribution of cross-sectional area as the basic wing-body configuration, model A. Model E was a 0.1538-scale model of the larger models and will be referred to as the small body with bump.

TESTS AND MEASUREMENTS

All the models were tested at the Langley Pilotless Aircraft Research Station at Wallops Island, Va. Models A to D were propelled from zero-length launchers by fin-stabilized 6-inch ABL Deacon rocket motors (fig. 4) to supersonic speeds. After burnout of the rocket motors, the models separated from the boosters and decelerated through the test Mach number range. Velocity and trajectory data were obtained from the CW Doppler velocimeter and the NACA modified SCR 584 tracking radar unit, respectively. A survey of atmospheric conditions including winds aloft was made by radiosonde measurements from an ascending balloon that was released at the time of each launching.

The flight tests covered continuous ranges of Mach number varying between Mach numbers 0.8 and 1.6. The corresponding Reynolds numbers for models A to D varied from approximately 4×10^6 to about 12×10^6, based on wing mean aerodynamic chord, as is shown in figure 5. Since no transonic data were obtained from model D, a small-scale configuration, model E, was flight tested at transonic speeds to provide data in this speed range for the body with bump. Model E was tested using the Langley helium gun (at the testing station at Wallops Island, Va.) which is described in reference 3 and covered a continuous Mach number range from about 0.85 to 1.3 with corresponding Reynolds number range varying from 1.3×10^6 to 2×10^6 (fig. 5), based on the scaled down mean aerodynamic chord of the wing.

The values of total drag coefficient, based on the total wing planform area, for all the models were obtained during decelerating flight with the expression

$$C_D = - \frac{W}{qgS_w} (a + g \sin \gamma)$$

where a was obtained by differentiating the velocity-time curve from the CW Doppler velocimeter. A more complete discussion of the method for reducing the data is given in reference 8.

The total drag coefficient for the bodies of revolution, based on the frontal area of the parabolic body, was obtained from

$$C_{D_f} = C_D \frac{S_w}{S_f}$$

where $S_w/S_f = 16.5$.

The error in total drag coefficient C_D was estimated to be less than ±0.0005 at supersonic speeds and less than ±0.001 at transonic speeds. The Mach numbers were determined within ±0.005 throughout the test range.

RESULTS AND DISCUSSION

The variations of total drag coefficient C_D for the wing-body configurations and C_{D_f} for the equivalent bodies of revolution with Mach

number are given in figure 6. A comparison of C_{D_f} for the two similar configurations with the bump, models D and E, is shown in figure 6(d). The adjusted curve in figure 6(d) was obtained by correcting the values of C_{D_f} from model E for the difference in Reynolds number between the two similar bodies, thus giving the variations of C_{D_f} with M for model D throughout the test range. Reference 9 was used to determine the friction drag coefficients of models D and E.

In figure 7, the total drag coefficients of all the models are based on the total plan-form area of the wing and are compared between Mach numbers 0.8 and 1.6. The drag of the fins as obtained from reference 10 is presented also in this figure. In regards to models A and B, it should be noted that part of the difference in their subsonic drags may be due to the different surface finishes (see fig. 3) of the wings as is indicated in reference 11. Although the indentation reduced the total drag of the basic wing-body-fin combination throughout most of the transonic and supersonic Mach number range, the savings in drag due to indenting the body was obtained at the penalty of reducing the volume of the body by 24 percent or of the wing-body combination by 19 percent. The drag from the two bodies of revolution (models C and D) were approximately the same at subsonic speeds, but model D with the bump had more drag at supersonic speeds because of its body shape and lower fineness ratio than model C.

In order to determine the effectiveness of the transonic area rule for determining or reducing the drag rise of the present configuration, the drag rises of the models tested are presented in figure 8(a) for comparison with the normal cross-sectional area distributions of the models in figure 2. The transonic area rule of reference 1 states that the zero-lift drag rise of thin, low-aspect-ratio wing-body combinations near the speed of sound is primarily dependent on the axial distribution of cross-sectional area of the configuration and that the drag rise of any such configuration is approximately the same as that of its equivalent body of revolution at Mach number 1.0. The results in figure 8(a) show that a relatively large difference in drag rise was obtained near and above Mach number 1 for the basic configuration (model A) and its equivalent body (model D). The drag rise of model D was about 40 percent lower than that of model A at Mach number 1.0 and even lower at supersonic speeds. The agreement between the indented configuration model B and its equivalent body model C was good at Mach number 1 with increasingly poorer agreement as the Mach number was increased to the limit of the tests. These results are similar to those obtained from an earlier flight test investigation (ref. 2) of the transonic area rule for a 45° sweptback-wing—cylindrical-body configuration as is shown in figure 8(b) and also the sweptback-wing test results of references 1 and 3. Tests of other wing-body configurations with delta wings and straight wings in references 1 and 3 show that better agreement between the drag rises of the

configurations and their equivalent bodies of revolution may be obtained. Although the sweptback wings tested herein were thin and had a low aspect ratio and taper ratio, as specified by the transonic area rule, it appears that the area rule does not work as well for swept wings as it does for delta and straight wings.

Of particular interest is the effect the indentations have on the drag rise of the configurations at transonic and supersonic speeds. By indenting the body of the basic configuration to reduce the normal cross-sectional area to that of the original body alone and make the area distribution smooth, the drag rise was reduced between Mach numbers 0.9 and 1.35 for the present tests (fig. 8(a)) and between 0.95 and 1.18 for the tests in reference 2, (fig. 8(b)). Although the drag rises of the equivalent bodies did not match that of their wing-body combinations, indenting the body according to the transonic area rule did give a good reduction in the drag rise at transonic speeds.

The comparisons in figure 8 also show that the beneficial effect of the transonic indentation decreased as the Mach number increased and then the drag rise exceeded that from the original configuration. At Mach number 1.5 for the present tests, the pressure drag was increased by about 10 percent with the indentation. For the configuration of reference 2, the indentation increased the drag rise by 25 percent above $M = 1.3$. Tests of delta-wing configurations with body contouring according to the transonic area rule in references 6 and 12 also show that the favorable effects from the indentation decreased with increasing Mach number up to Mach number 2.0. These comparisons and unpublished data for straight-wing configurations indicate that while such indentations are beneficial at transonic speeds they can be harmful at higher speeds.

With the aid of the supersonic area rule of references 13 and 14, it is possible to show that the transonic indentations have an undesirable effect on the wave drag at supersonic speeds. The supersonic area rule (ref. 14) is an extension of the transonic area rule in that it involves the consideration of a series of cross-sectional area distributions instead of just the normal area distribution. Each area distribution of the series is obtained from the area intercepted by parallel Mach planes at a given angle of roll of the configuration with respect to the Mach planes. According to the convention used, the Mach planes are perpendicular to the wing plane at 0° of roll. For the symmetrical models of this investigation, roll angles from 0° to 90° must be considered. For the present wing-body configurations, models A and B, the cross-sectional area distributions have been determined for roll angles of 0°, 45°, and 90° at $M = 1.50$, and for a roll angle of 0° at $M = 1.38$. These areas, including the average area for the three roll angles at $M = 1.50$, are presented in figure 9, except for the areas at 90° roll angle. For this last case, it should be noted that the areas at 90° roll angle for the symmetrical models A and B remain essentially the same for the Mach number range considered and are shown in figure 2. Also, it has been assumed that the body area distribution does not change with Mach number.

A comparison of the area distributions at the three roll angles for M = 1.50 in figures 2 and 9, show that the area distributions of both models A and B improve as the models are rolled from 0° to 90°. For the present case, it is difficult to determine which configuration has the greater pressure drag from either comparing the areas at the individual roll angles or the average areas. In this regard, it would be necessary to compute the drag coefficients of the equivalent bodies of revolution at each roll angle (ref. 14) and average them to obtain the total drag.

An indication of the effect of increasing Mach number on the drag is given in figures 2 and 9 by comparing the area distribution at 0° roll angle. It is clearly shown that the area distribution of the indented configuration becomes worse as the Mach number is increased to M = 1.50. At higher Mach numbers, the dent in the area distribution for model B would become even more pronounced, indicating that the indentation would eventually produce a greater pressure drag for model B than is obtained from the unmodified configuration model A.

CONCLUSIONS

The results of an investigation of the transonic area rule by rocket-model tests of zero-lift models of a 52.5° sweptback wing-body combination with and without a fuselage indentation and of their corresponding equivalent bodies of revolution between Mach numbers 0.8 and 1.6 indicate the following conclusions:

1. Indenting the fuselage of the wing-body combination, in order to reduce the normal cross-sectional area distribution to that of the original body alone, reduced the drag rise between Mach numbers 0.9 and 1.35 and increased the drag rise above Mach number 1.35.

2. Near Mach number 1.0, approximately the same drag rise was obtained from the wing-body combination with indentation and its equivalent body of revolution or the original fuselage alone. The drag rise from the equivalent body of revolution with the bump corresponding to the sweptback wing was only 60 percent of that for the basic wing-body configuration at the speed of sound.

3. The maximum drag rise of the wing-body combinations was not duplicated by their equivalent bodies of revolution.

Langley Aeronautical Laboratory,
National Advisory Committee for Aeronautics,
Langley Field, Va., August 2, 1954.

REFERENCES

1. Whitcomb, Richard T.: A Study of the Zero-Lift Drag-Rise Characteristics of Wing-Body Combinations Near the Speed of Sound. NACA RM L52H08, 1952.

2. Hoffman, Sherwood: An Investigation of the Transonic Area Rule by Flight Tests of a Sweptback Wing on a Cylindrical Body With and Without Body Indentation Between Mach Numbers 0.9 and 1.8. NACA RM L53J20a, 1953.

3. Hall, James Rudyard: Comparison of Free-Flight Measurements of the Zero-Lift Drag Rise of Six Airplane Configurations and Their Equivalent Bodies of Revolution at Transonic Speeds. NACA RM L53J21a, 1954.

4. Robinson, Harold L.: A Transonic Wind-Tunnel Investigation of the Effects of Body Indentation, As Specified by the Transonic Drag-Rise Rule, on the Aerodynamic Characteristics and Flow Phenomena of a 45° Sweptback-Wing—Body Combination. NACA RM L52L12, 1953.

5. Carmel, Melvin M.: Transonic Wind-Tunnel Investigation of the Effects of Aspect Ratio, Spanwise Variations in Section Thickness Ratio, and a Body Indentation on the Aerodynamic Characteristics of a 45° Sweptback Wing-Body Combination. NACA RM L52L26b, 1953.

6. Whitcomb, Richard T.: Recent Results Pertaining to the Application of the "Area Rule." NACA RM L53I15a, 1953.

7. Hopko, Russell N., Piland, Robert O., and Hall, James R.: Drag Measurements at Low Lift of a Four-Nacelle Airplane Configuration Having a Longitudinal Distribution of Cross-Sectional Area Conducive to Low Transonic Drag Rise. NACA RM L53E29, 1953.

8. Wallskog, Harvey A., and Hart, Roger G.: Investigation of the Drag of Blunt-Nosed Bodies of Revolution in Free Flight at Mach Numbers From 0.6 to 2.3. NACA RM L53D14a, 1953.

9. Van Driest, E. R.: Turbulent Boundary Layer in Compressible Fluids. Jour. Aero. Sci., vol. 18, no. 3, Mar. 1951, pp. 145-160, 216.

10. Morrow, John D., and Nelson, Robert L.: Large-Scale Flight Measurements of Zero-Lift Drag of 10 Wing-Body Configurations at Mach Numbers From 0.8 to 1.6. NACA RM L52D18a, 1953.

11. Bingham, Gene J., and Braslow, Albert L.: Subsonic Investigation of Effects of Body Indentation on Zero-Lift Drag Characteristics of a 45° Sweptback Wing-Body Combination With Natural and Fixed Boundary-Layer Transition Through a Range of Reynolds Number from 1×10^6 to 8×10^6. NACA RM L54B18a, 1954.

12. Carlson, Harry W.: Preliminary Investigation of the Effects of Body Contouring As Specified by the Transonic Area Rule on the Aerodynamic Characteristics of a Delta Wing-Body Combination at Mach Numbers of 1.41 and 2.01. NACA RM L53G03, 1953.

13. Whitcomb, Richard T., and Fischetti, Thomas L.: Development of a Supersonic Area Rule and an Application to the Design of a Wing-Body Combination Having High Lift-to-Drag Ratios. NACA RM L53H31a, 1953.

14. Jones, Robert T.: Theory of Wing-Body Drag at Supersonic Speeds. NACA RM A53H18a, 1953.

TABLE I.- COORDINATES OF NACA 65A004 AIRFOIL

Station, percent chord	Ordinate, percent chord
0	0
.5	.311
.75	.378
1.25	.481
2.5	.656
5.0	.877
7.5	1.062
10	1.216
15	1.463
20	1.649
25	1.790
30	1.894
35	1.962
40	1.996
45	1.996
50	1.952
55	1.867
60	1.742
65	1.584
70	1.400
75	1.193
80	.966
85	.728
90	.490
95	.249
100	.009
L. E. radius: 0.102. T. E. radius: 0.010.	

TABLE II.- COORDINATES OF PARABOLIC BODY

[Stations measured from body nose]

Station, in.	Ordinate, in.
0	0
1	.245
2	.481
4	.923
6	1.327
10	2.019
14	2.558
18	2.942
22	3.173
26	3.250
30	3.233
34	3.181
38	3.095
42	2.975
46	2.820
50	2.631
54	2.407
58	2.149
62	1.857
65	1.615

TABLE III.- COORDINATES OF BODY WITH INDENTATION

[Stations measured from body nose]

Station, in.	Ordinate, in.
(a)	(a)
28	3.246
30	3.176
32	3.073
34	2.934
36	2.748
38	2.619
40	2.455
42	2.341
44	2.262
46	2.243
48	2.238
50	2.297
52	2.292
54	2.251
56	2.221
58	2.149
60	2.007
62	1.857
64	1.698
65	1.615

[a]Coordinates between stations 0 and 28 are identical to those of the parabolic body.

TABLE IV.- COORDINATES OF BODY WITH BUMP[a]

[Stations measured from body nose]

Station, in.	Ordinate, in.
(b)	(b)
28	3.246
30	3.287
32	3.336
34	3.394
36	3.468
38	3.478
40	3.492
42	3.468
44	3.405
46	3.290
48	3.144
50	2.926
52	2.733
54	2.551
56	2.341
58	2.149
60	2.007
62	1.857
64	1.698
65	1.615

[a]Coordinates for the small body with bump are 0.1538-scale model of the above coordinates.

[b]Coordinates between stations 0 and 28 are identical to those of the parabolic body.

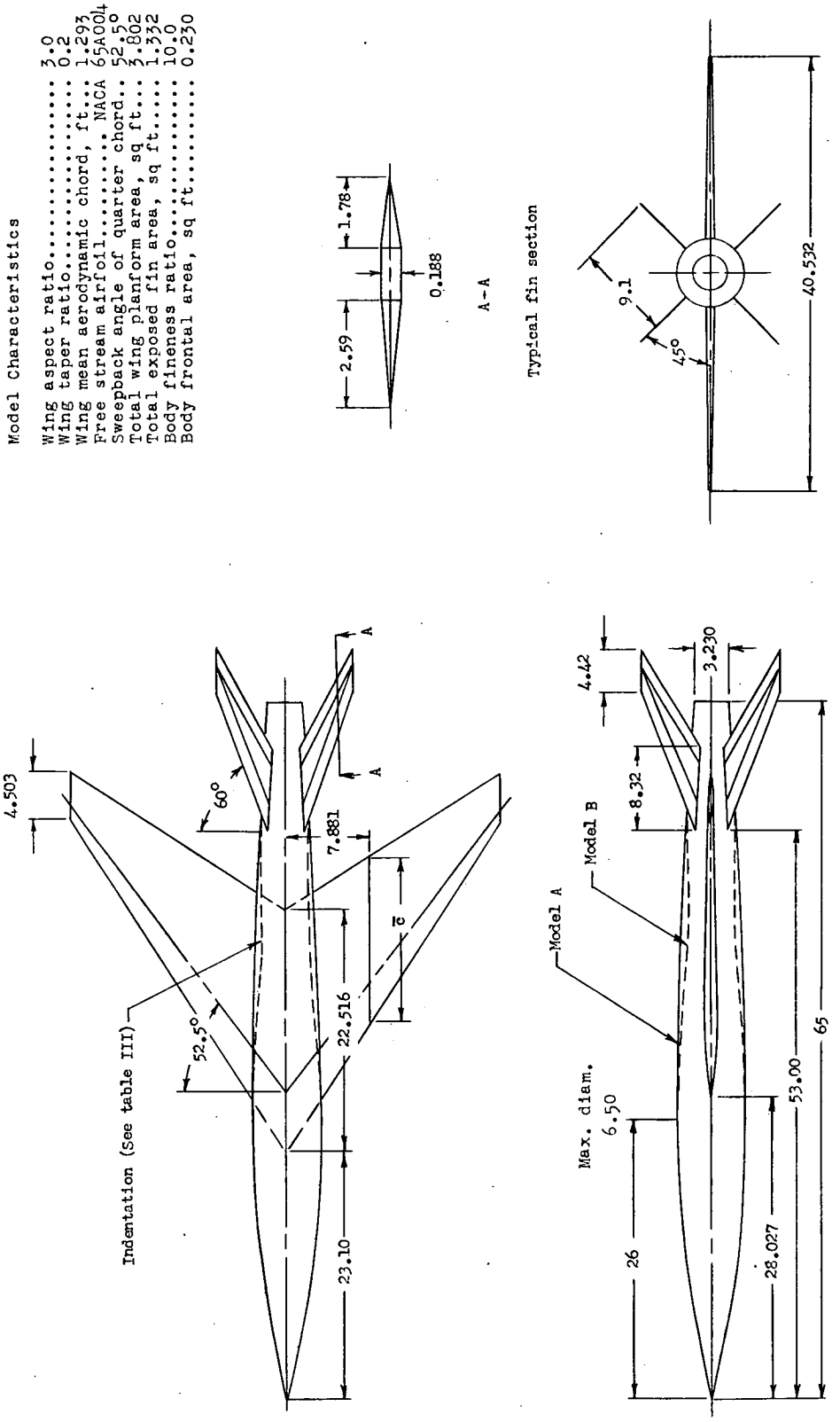

(a) Wing-body combinations. Models A and B.

Figure 1.- Details and dimensions of models tested. All dimensions are in inches.

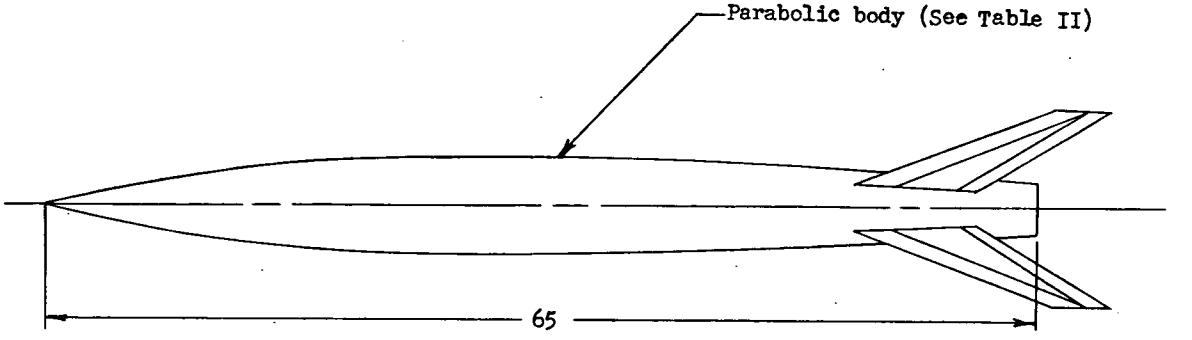

(b) Parabolic body. Model C; frontal area, 0.230 sq ft; fineness ratio, 10.

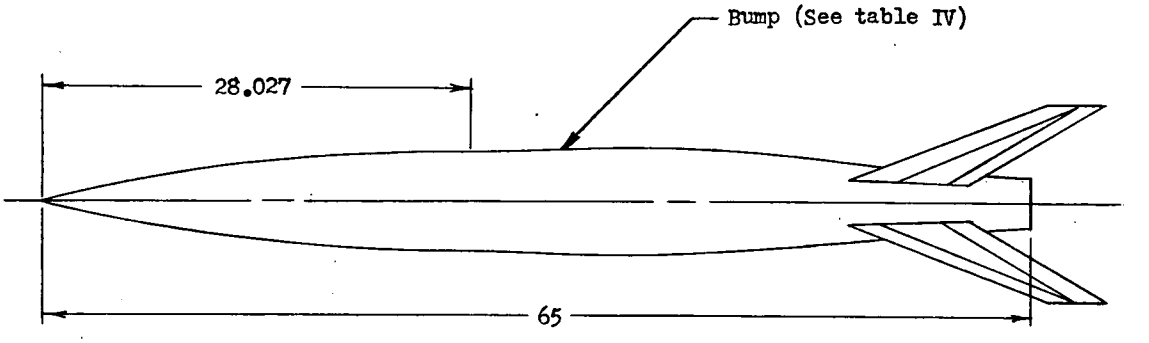

(c) Body with bump. Model D; frontal area, 0.266 sq ft; fineness ratio, 9.31.

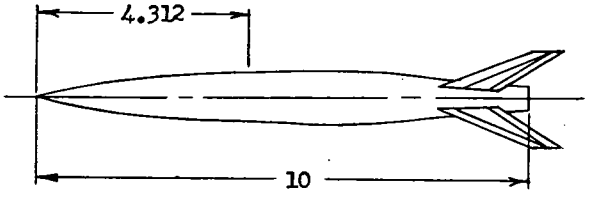

(d) Small body with bump. Model E; frontal area, 0.063 sq ft; fineness ratio, 9.31.

Figure 1.- Concluded.

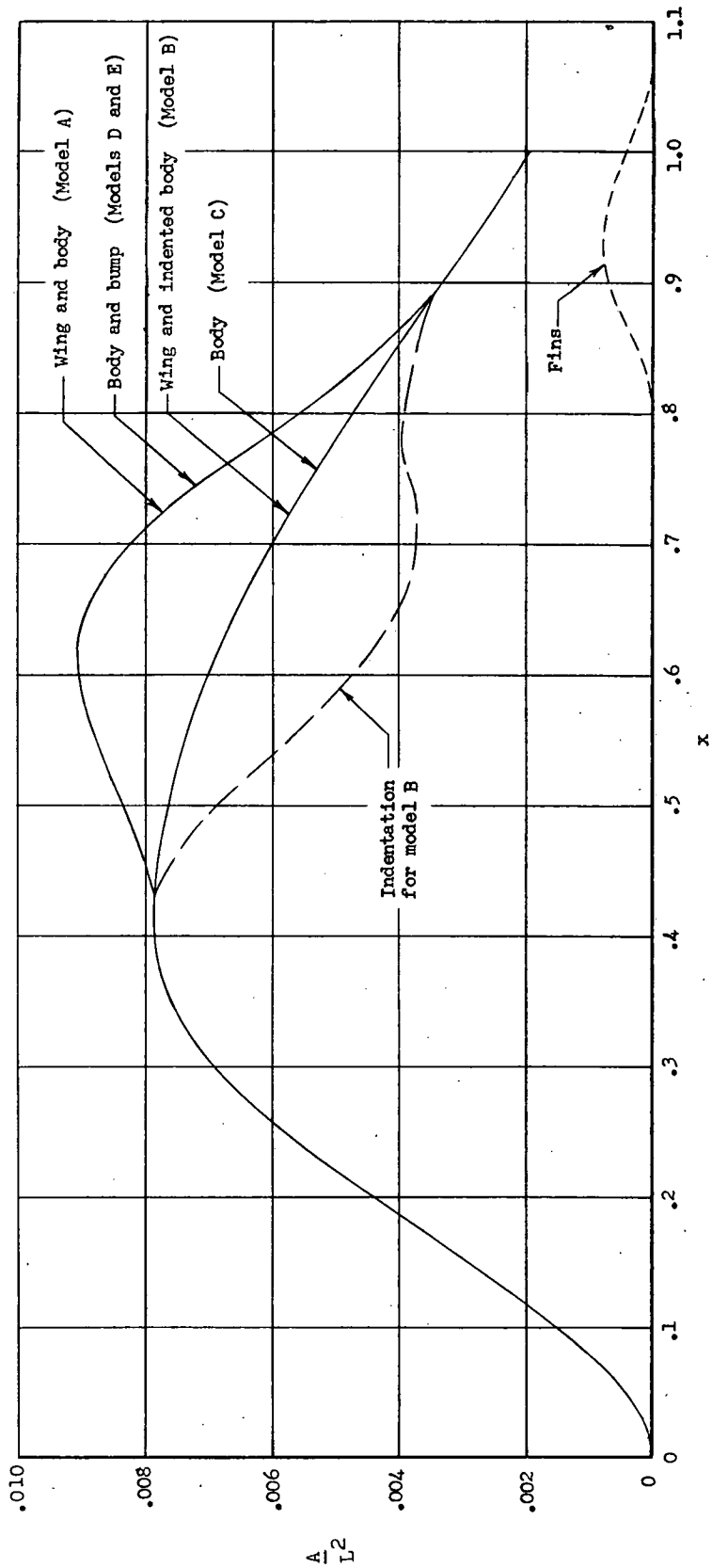

Figure 2.- Axial distribution of cross-sectional areas of models at any roll angle at Mach number 1.0 or at 90° rotation of each model with respect to the Mach planes at supersonic Mach numbers.

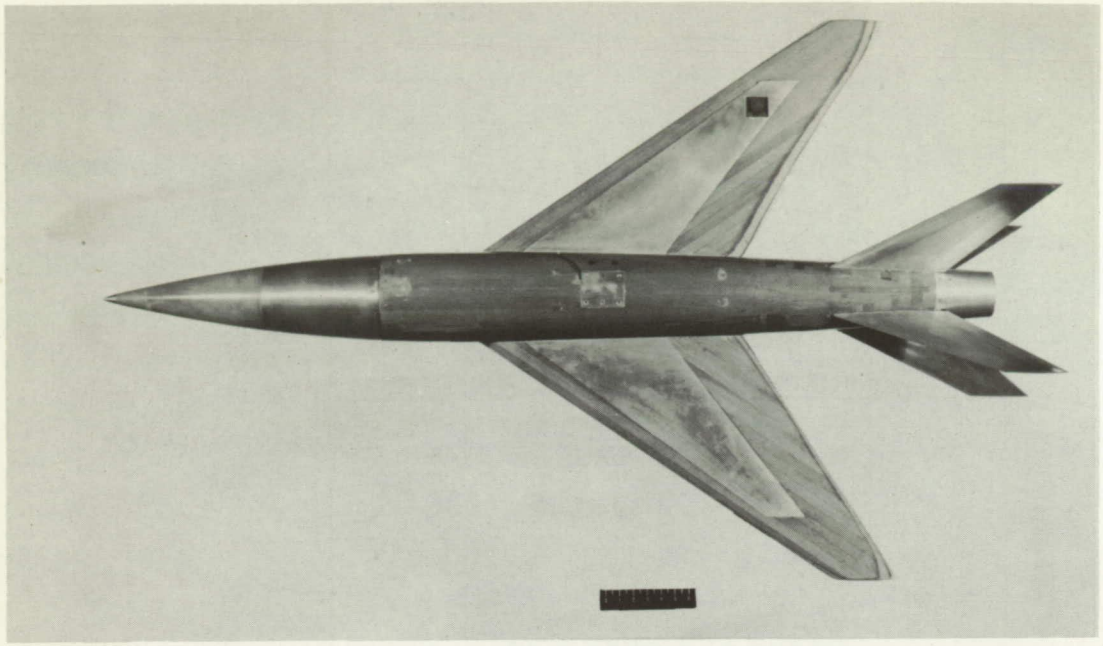

L-81355.1

(a) Wing and body. Model A.

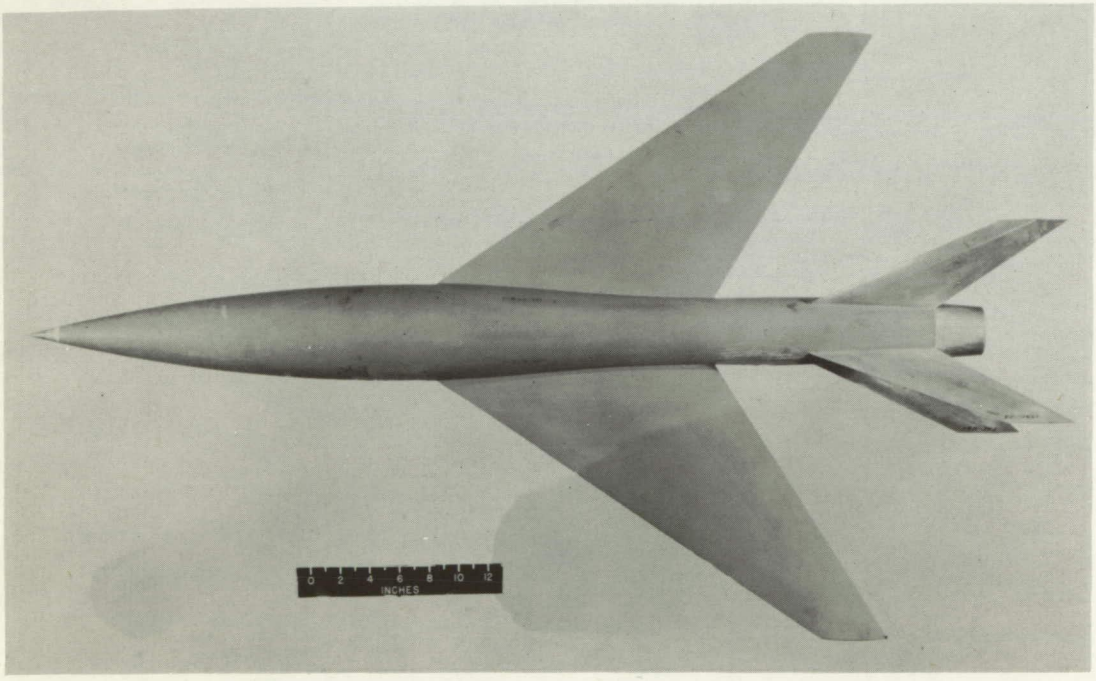

L-83377.1

(b) Wing and indented body. Model B.

Figure 3.- Photographs of models.

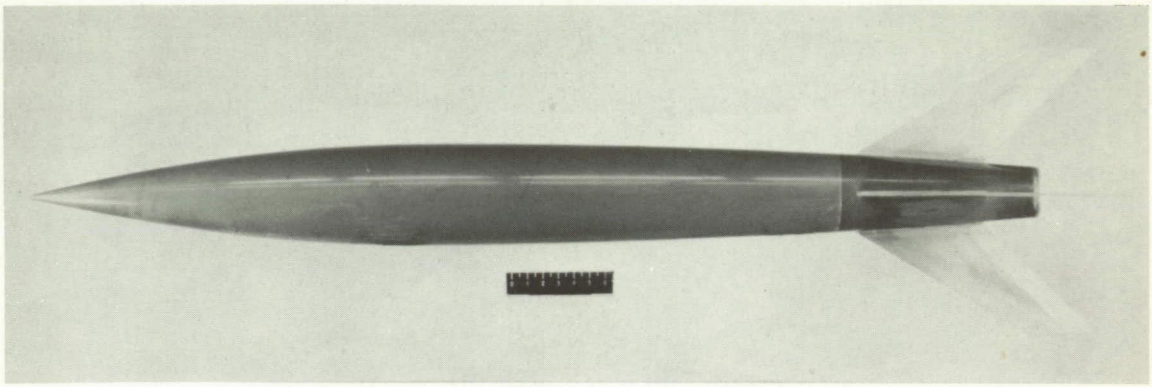

L-77566.1

(c) Parabolic body. Model C.

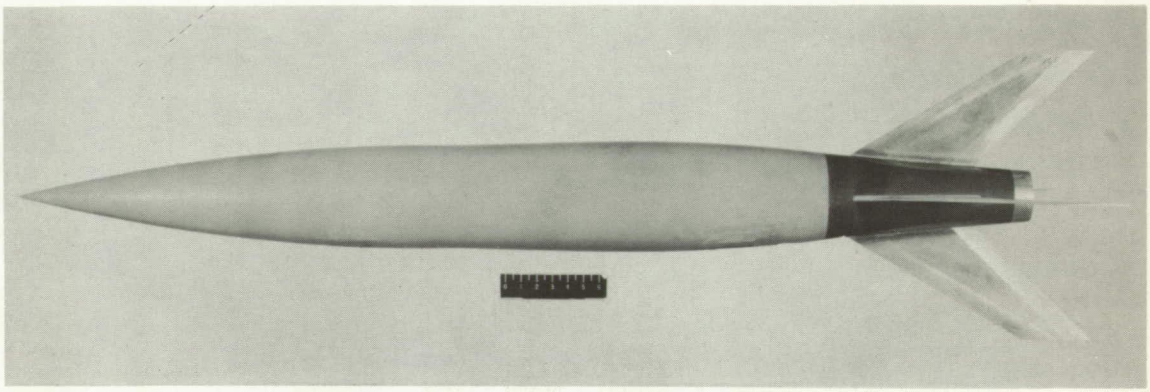

L-80460.1

(d) Body with bump. Model D.

Figure 3.- Continued.

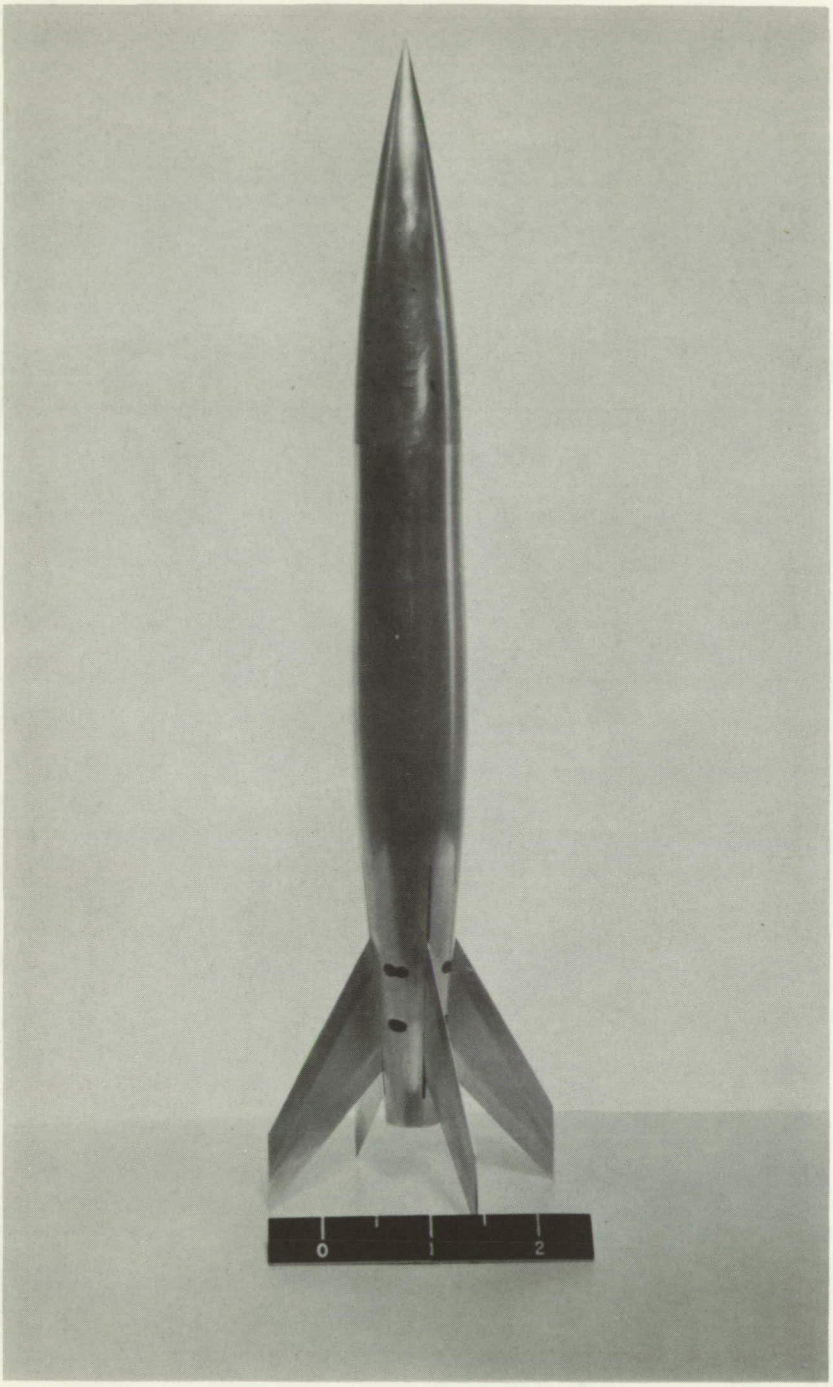

L-81979

(e) Small body with bump. Model E.

Figure 3.- Concluded.

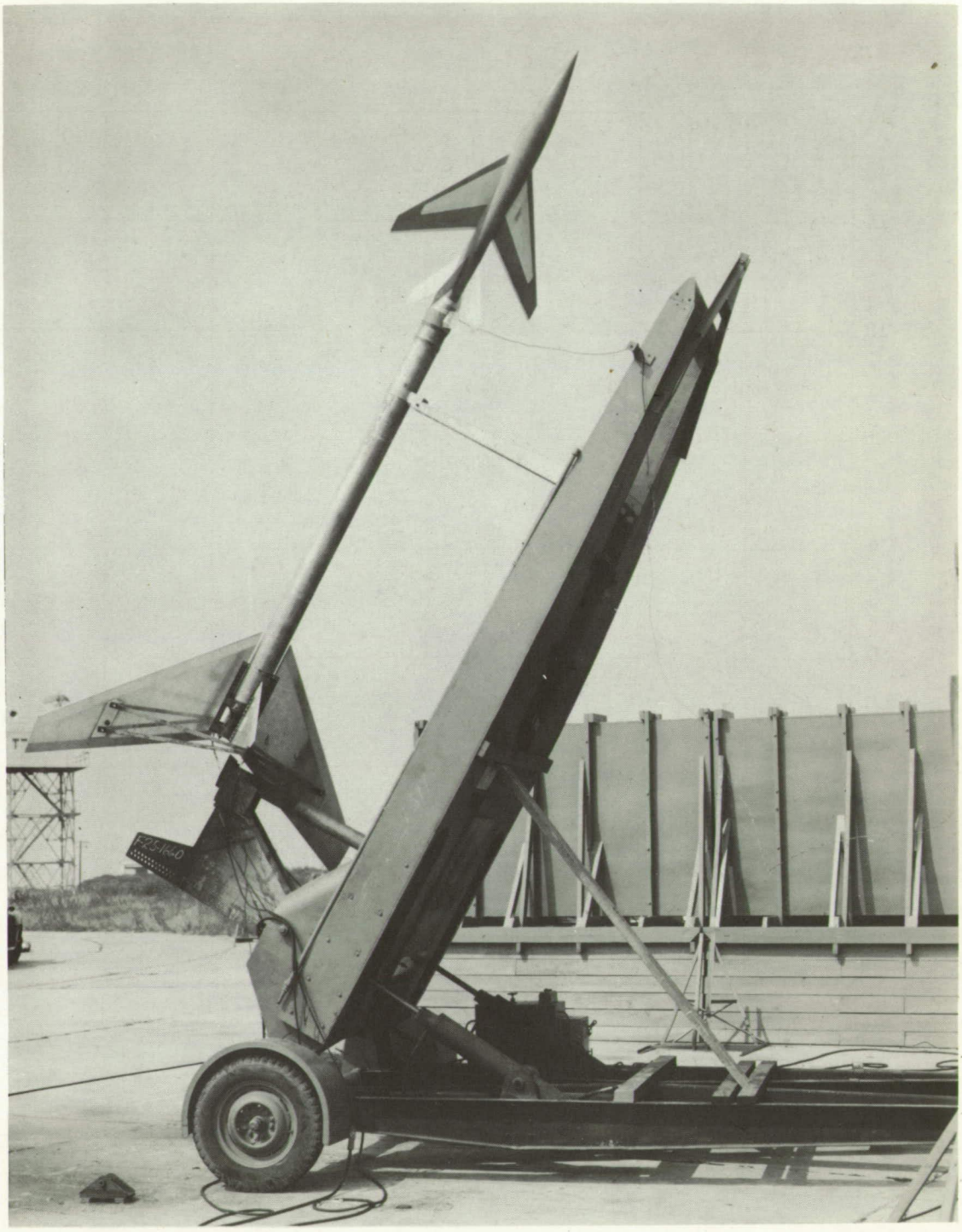

L-81052

Figure 4.- A model and booster on zero-length launcher.

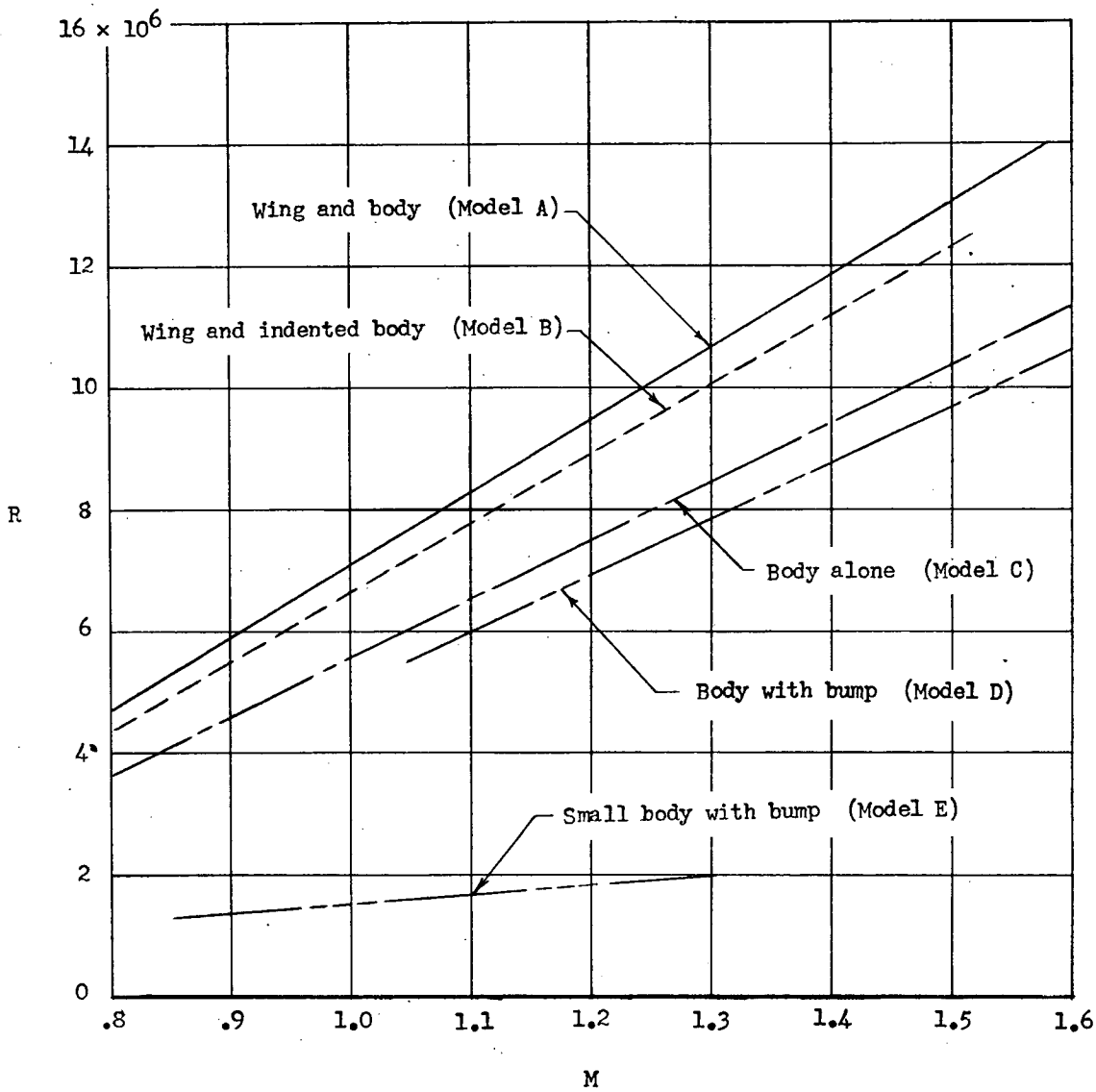

Figure 5.- Variation of Reynolds number with Mach number for models tested. Reynolds number is based on wing mean aerodynamic chord.

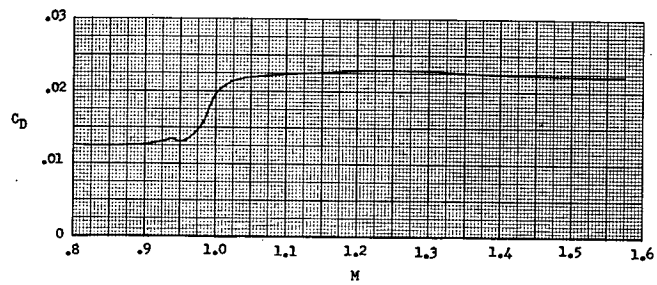

(a) Wing and body. Model A.

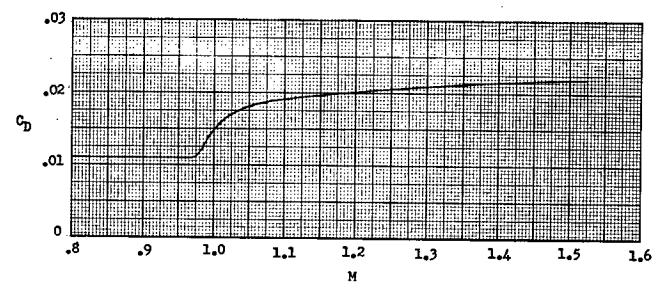

(b) Wing and indented body. Model B.

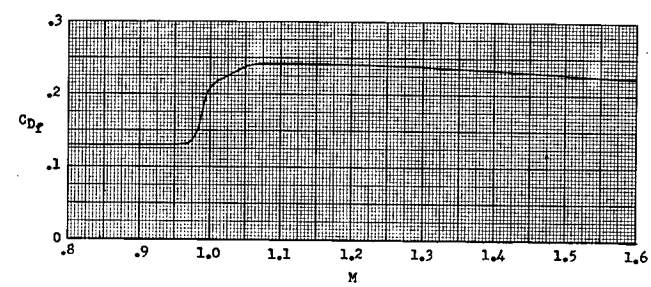

(c) Body alone. Model C.

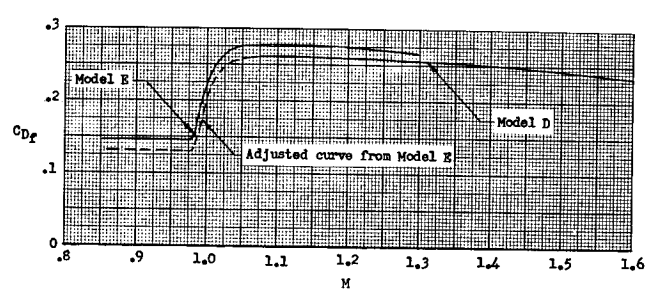

(d) Body with bump. Models D and E.

Figure 6.- Variation of total drag coefficient with Mach number for models tested.

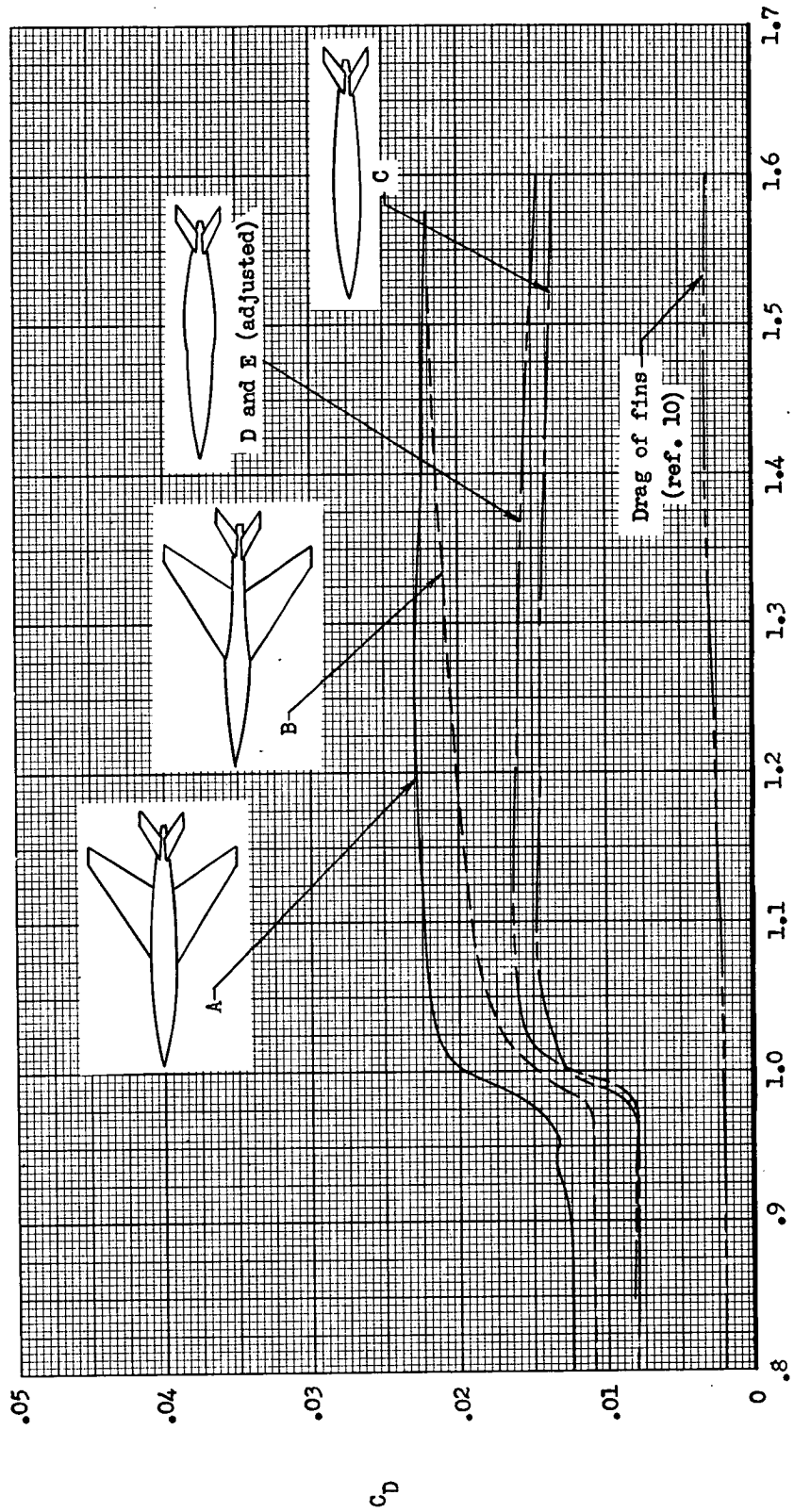

Figure 7.- Comparison of the variations of total drag coefficient with Mach number for the models tested.

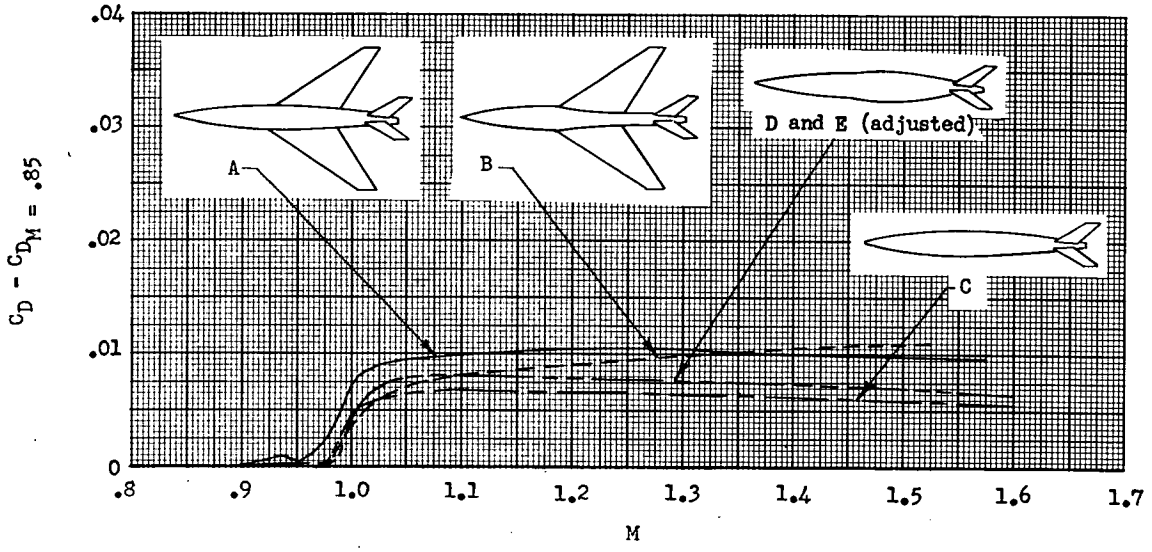

(a) Models tested.

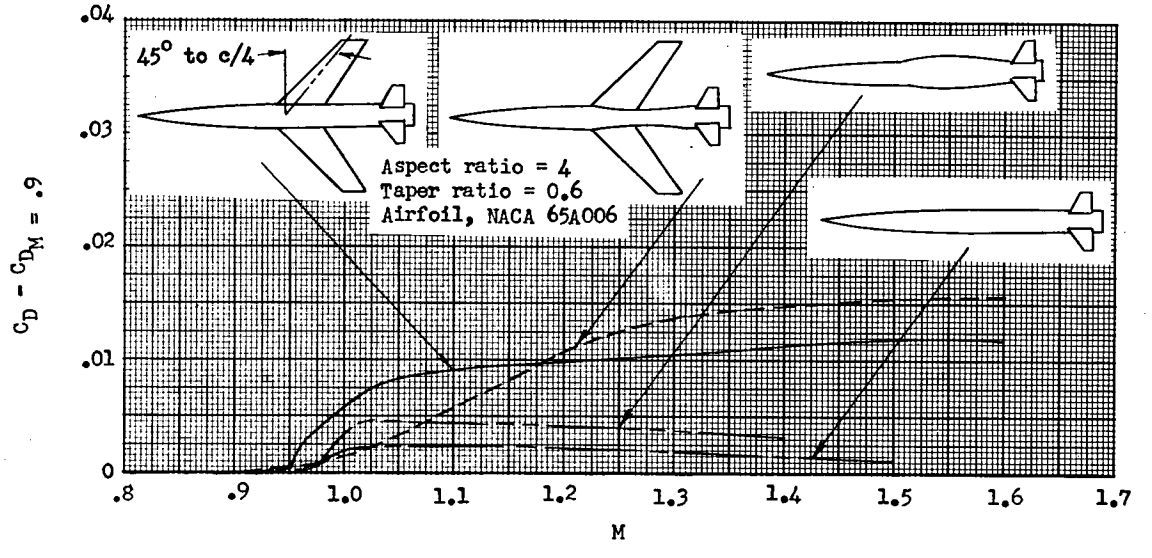

(b) Models of reference 2.

Figure 8.- Comparison of the drag-rise coefficients for the models tested and the models of reference 2.

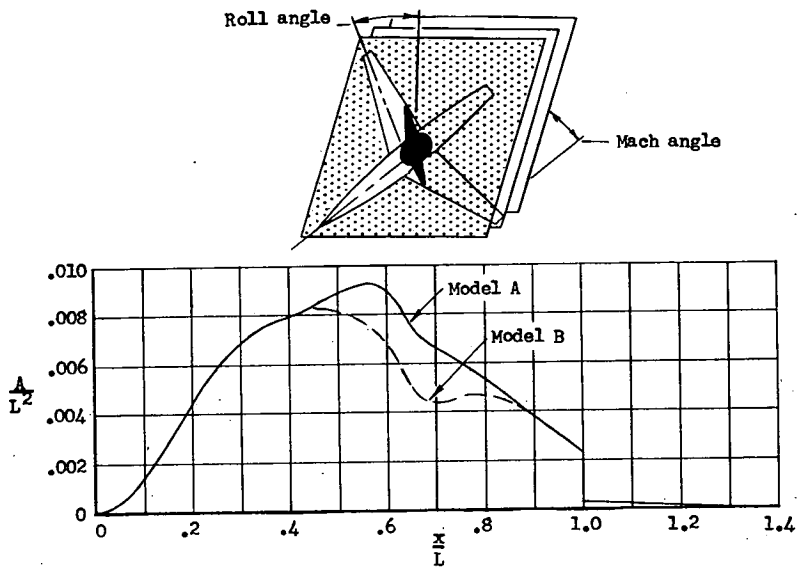

(a) Roll angle of 0° at M = 1.50.

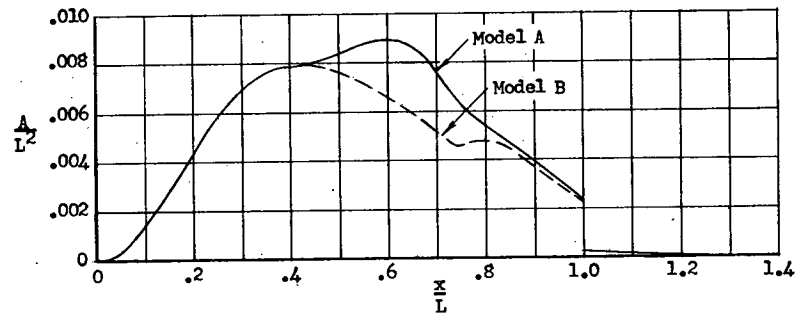

(b) Roll angle of 0° at M = 1.38 or roll angle of 45° at M = 1.50.

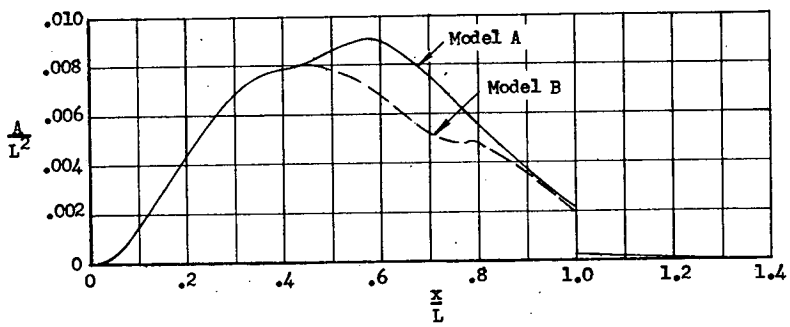

(c) Average for roll angles of 0°, 45°, and 90° at M = 1.50.

Figure 9.- Comparison of the area distributions of the wing-body combinations with and without indentation as obtained by oblique area cuts at supersonic Mach numbers.

NACA-Langley - 11-19-54 - 425